Available online at www.sciencedirect.com
ScienceDirect
Biochemical and Biophysical Research Communications 358 (2007) 7–11
BBRC
www.elsevier.com/locate/ybbrc

Development of potent inhibitors of the coxsackievirus 3C protease

Eui Seung Lee [a], Won Gil Lee [a], Soo-Hyeon Yun [b], Seong Hwan Rho [a], Isak Im [a], Sung Tae Yang [a], Saravanan Sellamuthu [a], Yong Jae Lee [a], Sun Jae Kwon [c], Ohkmae K. Park [c], Eun-Seok Jeon [b], Woo Jin Park [a,*], Yong-Chul Kim [a,*]

[a] *Department of Life Science, Gwangju Institute of Science and Technology, 1 Oryong-dong, Buk-gu, Gwangju 500-712, Republic of Korea*
[b] *Department of Medicine, Sungkyunkwan University School of Medicine, Cardiac and Vascular Center, Samsung Medical Center, Seoul 135-710, Republic of Korea*
[c] *School of Life Science and Biotechnology, Korea University, Seoul 136-701, Republic of Korea*

Received 9 March 2007
Available online 20 April 2007

Abstract

Coxsackievirus B3 (CVB3) 3C protease (3CP) plays essential roles in the viral replication cycle, and therefore, provides an attractive therapeutic target for treatment of human diseases caused by CVB3 infection. CVB3 3CP and human rhinovirus (HRV) 3CP have a high degree of amino acid sequence similarity. Comparative modeling of these two 3CPs revealed one prominent distinction; an Asn residue delineating the S2′ pocket in HRV 3CP is replaced by a Tyr residue in CVB3 3CP. AG7088, a potent inhibitor of HRV 3CP, was modified by substitution of the ethyl group at the P2′ position with various hydrophobic aromatic rings that are predicted to interact preferentially with the Tyr residue in the S2′ pocket of CVB3 3CP. The resulting derivatives showed dramatically increased inhibitory activities against CVB3 3CP. In addition, one of the derivatives effectively inhibited the CVB3 proliferation *in vitro*.

Keywords: Coaxsackievirus; 3C protease; Inhibitor

Coxsackievirus B3 (CVB3), a member of the picornavirus family, is a primary causative agent of viral myocarditis in humans [1–3]. Acute myocarditis is a principle cause of heart failure in children and adolescents, and often progresses to chronic myocarditis and dilated cardiomyopathy, which are responsible for approximately 50% of the heart transplantations registered annually worldwide [4,5]. No effective antiviral therapies for either prevention or treatment of the diseases caused by CVB3 infection are currently available. Like other picornaviruses including polioviruses, human rhinoviruses (HRV), and hepatitis A virus, the positive strand RNA genome of CVB3 is translated into a large polyprotein precursor which undergoes a series of proteolytic cleavages to generate functional viral proteins. Processing of the polyprotein is essential for the production of new, infectious virions, and is primarily dependent on two virally encoded proteases 2A and 3C [2,4,6]. Therefore, these enzymes are attractive therapeutic targets for development of antiviral therapeutic agents [7].

In this study, we sought to develop potent inhibitors of CVB3 3C protease (3CP). CVB3 3CP is highly homologous to HRV 3CP in their amino acids sequences (approximately 64%). Utilizing information from the crystal structure of HRV 3CP [8,9] in complex with its inhibitor, AG7088 [10], and the comparatively modeled structure of CVB3 3CP, we rationally designed various AG7088 derivatives. We report here that several derivatives are indeed highly potent inhibitors of CVB3 3CP, and that one of the compounds was highly effective in preventing proliferation of CVB3 *in vitro*.

* Corresponding authors. Fax: +82 62 970 2484.
E-mail addresses: wjpark@gist.ac.kr (W.J. Park), yongchul@gist.ac.kr (Y.-C. Kim).

0006-291X/$ - see front matter © 2007 Elsevier Inc. All rights reserved.
doi:10.1016/j.bbrc.2007.03.208

Materials and methods

Comparative modeling of CVB3 3CP. A model for the structure of CVB3 3CP was generated based on information from the structure of HRV 3CP [8,9] in complex with the inhibitor AG7088 (PDB# 1CQQ) [10]. The two 3CPs have a high degree of amino acid sequence similarity. Modeling was performed using MODELLER software [11]. The model with the lowest MODELLER restraint energy was further refined by energy minimization using GROMACS software [12].

Synthesis of inhibitors. All reagents used for inhibitor synthesis were purchased from Sigma–Aldrich. The synthetic scheme for the CVB3 3CP inhibitors is outlined in Fig. 2 [13]. Alcoholic compounds **1** (3.06 mmol, 2.0 equiv) was added to a solution of diethylphosphonoacetic acid (1.53 mmol, 1.0 equiv) and PyBOP (2.30 mmol, 1.5 equiv) in dichloromethane (30 ml) at room temperature (RT), and the mixture was stirred for 2 h. After concentrating the solution by evaporation of dichloromethane, the resulting solution was partitioned between ethyl acetate (30 ml) and de-ionized water (2 × 20 ml). The combined organic layers were dried over Na_2SO_4, filtered, concentrated under reduced pressure, and purified by silica gel column chromatography (40% EtOAc in hexane) to yield compounds **2a**–**f** (>50.0%).

Sodium bis(trimethylsilyl)amide (1.0 M solution in THF, 0.67 mmol, 1.5 equiv) was added to a solution of compound **2** (0.54 mmol, 1.2 equiv) in THF (20 ml) at −78 °C, and the mixture was stirred for 20 min. Compound **3** [13] was added to the mixture, and stirring was continued for 2 h at the same temperature. The solution was then warmed to 0 °C for 10 min, and then partitioned between 0.5 M HCl (20 ml) and a 1:1 mixture of hexane and EtOAc (2 × 20 ml). The combined organic layers were dried over Na_2SO_4, filtered, concentrated under reduced pressure, and purified by silica gel column chromatography (33% EtOAc in hexane) to yield compounds **4a**–**f** (>60.0%).

A solution of L-valine (15.74 mmol, 1.0 equiv), 5-methylisoxazole-3-carboxylic acid (15.74 mmol, 1.0 equiv), and PyBop (15.74 mmol, 1.0 equiv) in DMF (100 ml) was stirred for 5 h at 40 °C. After concentrating the solution by evaporation of DMF under vacuum, the mixture was partitioned between 1.0 M HCl (50 ml) and EtOAc (2 × 80 ml). The combined organic layers were dried over Na_2SO_4, filtered, concentrated under reduced pressure, and purified by silica gel column chromatography (3.0% MeOH in chloroform) to yield compound **5** (76.4%).

A solution of 4-fluoro-Phe-methyl ester (1.00 mmol, 1.0 equiv), compound 5 (1.00 mmol, 1.0 equiv), and PyBop (1.52 mmol, 1.5 equiv) in dichloromethane (20 ml) was stirred at RT for 2 h. After concentrating the solution by evaporation of dichloromethane, the mixture was partitioned between ethyl acetate (2 × 20 ml) and de-ionized water (20 ml). The combined organic layers were dried over Na_2SO_4, filtered, concentrated under reduced pressure, and purified by silica gel column chromatography (33% EtOAc in hexane) to yield compound **6** (80.3%), which was subsequently hydrolyzed in 1 N NaOH in MeOH (20 ml) to yield compound **7** (93%).

To remove the Boc group of compounds **4a**–**f**, 4 N HCl in 1,4-dioxane (5 ml) was added to a solution of compounds **4a**–**f** (0.15 mmol, 1.0 equiv) in the same solvent (5 ml) at RT. After 3 h, the solvent was evaporated under reduced pressure. Dichloromethane (10 ml) was added to the resulting residue containing compound **7** (0.15 mmol, 1.0 equiv). HOBt (0.45 mmol 3.0 equiv), DIPEA (0.90 mmol, 5.0 equiv), and EDC (0.45 mmol, 3.0 equiv) were added and the mixture was stirred overnight at RT. After concentrating the solution by evaporation of dichloromethane, the residue was partitioned between ethyl acetate (2 × 20 ml) and de-ionized water (20 ml). The combined organic layers were dried over Na_2SO_4, filtered, concentrated under reduced pressure, and purified by silica gel column chromatography (40% EtOAc in hexane) to yield compounds **8a**–**f** (>30.0%).

A solution of 20% TFA in dichloroethane was added to compounds **8a**–**f** (0.02 mmol, 1.0 equiv) at RT. After 1 h, the solvent was evaporated under reduced pressure, and compounds **9a**–**f** (>80.0%) were purified by preparative TLC (12% MeOH in chloroform).

Determination of the IC_{50} values of the inhibitors. The substrate peptide (TTLEALFQGPPVY) for CVB3 3CP was purchased from AnyGen (Gwangju, Korea). The CVB3 3CP coding region was amplified by PCR and subcloned into the pTYB12 expression vector (New England BioLabs). *Escherichia coli* strain BL21(DE3) was then transformed with the resulting plasmid. The CVB3 3CP was purified as previously described [14].

In the reaction buffer (40 mM Tris–HCl, pH 8.0, 1 mM dithiothreitol, and 0.1% Nonidet P-40), 150 μM substrate peptide, various concentrations of inhibitors, and 1 μM CVB3 3CP were added sequentially in a total volume of 100 μl, and then incubated for 1 h at 30 °C. Reactions were quenched by addition of 200 μl of 0.1% trifluoroacetic acid. A 200 μl aliquot of the mixture was subjected to reverse-phase HPLC on a 10 cm Vydac C_{18} column using a 0–95% 30 min linear gradient of acetonitrile in 0.1% trifluoroacetic acid. The CVB3 3CP activity in the absence of inhibitor was defined as 100%.

In vitro antiviral assay. HeLa-UVM cells were obtained from Sally Huber (University of Vermont) and maintained in Dulbecco's modified Eagle's medium (DMEM) supplemented with 10% fetal bovine serum. The H3 variant of the Woodruff strain of coxsackievirus B3 (CVB3-H3) was obtained from a cDNA copy [15]. Virus titers were determined using a plaque forming unit (pfu) assay on HeLa-UVM cells.

HeLa-UVM cells were infected with CVB3-H3 at a multiplicity of infection (MOI) of 100. CVB3 3CP inhibitors were added to the cultures at various final concentrations (0.5–100 μM) and incubated for 6–24 h. At the end of the incubation period, 15 μl of the proliferation-dye reagent which was supplied with Cell Counting Kit 8 (Dojindo Lab, Tokyo, Japan) was added. Only viable cells with intact mitochondria are stained with this reagent. Absorbance at 450 nm was measured using an ELISA plate reader. Non-infected HeLa-UVM cells were used as a control and proliferation of these cultures was defined as 100%. Data are presented as means ± SD from three independent experiments.

GFP detection and Western blot analysis. Previously, a GFP-CVB3 fusion gene was constructed in which a green fluorescent protein (GFP) gene was placed immediately upstream of theVP0 capsid protein of CVB3 with a cleavage site for CVB3 3CP positioned between GFP and VP0. GFP is cleaved from the viral polyprotein by 3CP during viral replication [16,17]. HeLa-UVM cells were infected with GFP-CVB3 (MOI, 100) for 6 h, and GFP expression was analyzed either by fluorescence microscopy or by Western blotting. The fluorescence of functional GFP in the infected cells was observed without fixation using the FITC filter on a fluorescence microscope. Total protein extracts from the cultures (10 μg) were fractionated on a 10% SDS–PAGE gel and then blotted onto Hybond-ECL membranes (Amersham). Protein bands with positive antibody reactions against GFP and tubulin were visualized by chemiluminescence (Amersham). GFP expression ($n = 4$) was quantified by densitometric analysis using ImageLab (version 2.2.4) and normalized to the control level (non-infected cells).

Results and discussion

Comparative modeling and synthesis of inhibitors

The structure of CVB3 3CP was modeled, and compared with that of HRV 3CP (Fig. 1). The conformation and amino acids demarcating the substrate binding pocket were found to be conserved in these proteases with the exception that Asn22 in HRV 3CP was replaced by Tyr22 in CVB 3CP. These amino acids appear to be critical for determining the P2′ specificity of the substrates [8,9]. AG7088 is a potent peptidomimetic inhibitor of HRV 3CP that was developed by structure-based drug design approaches [18], and is currently being evaluated in a Phase 1 clinical trial in humans [10]. This inhibitor is composed of a substrate-derived tri-peptide binding determinant with affinity for the target protease and a Michael acceptor

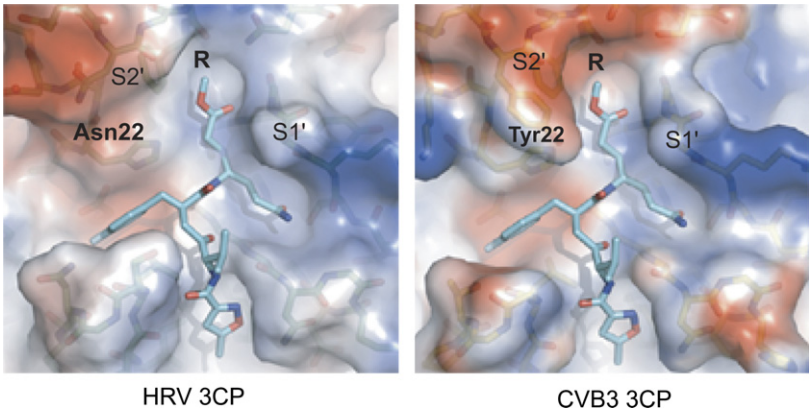

Fig. 1. Comparative modeling of CVB3 3CP. Modeling of CVB3 3CP was performed using the HRV 3CP structure as a reference. Structures of HRV 3CP and CVB3 3CP docked with a HRV 3CP inhibitor, AG7088, are shown. Note the presence of Tyr22 at S2′ of CVB3 3CP (right panel). We hypothesized that Tyr22 would interact preferentially with aromatic R groups in potential inhibitors. The electrostatic calculation of models and the figure preparation were performed using the PyMol software [19].

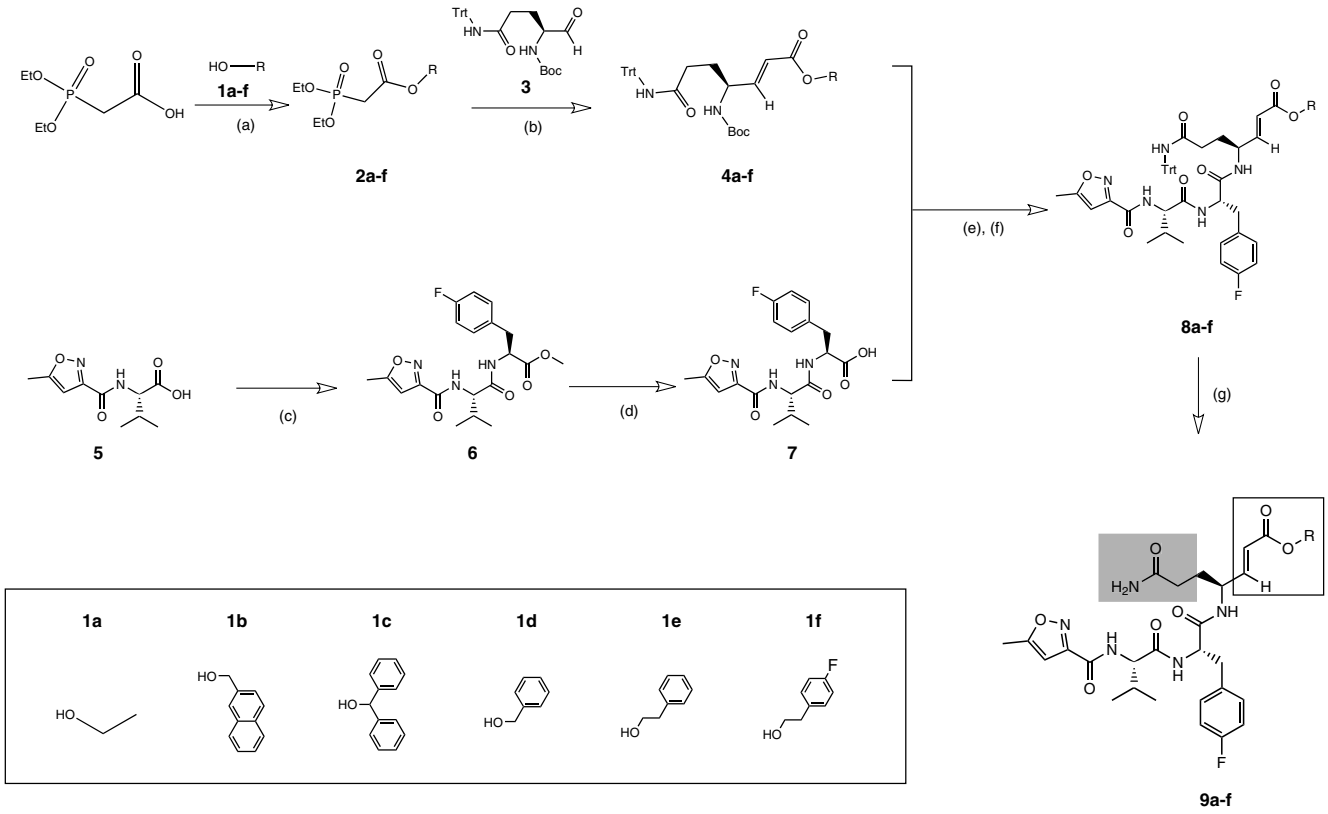

Fig. 2. Synthesis of CVB3 3CP inhibitors. Reagents and conditions are as follows: (Tr = CPh3) (a) 2.0 equiv of alcohol compound, 1.5 equiv of Pybop, DCM, 2 h, 56.3%; (b) 1.5 equiv of sodium bis(trimethylsilyl)amide, THF, −78 °C, 2 h, 63.0%; (c) 1.0 equiv of Boc-L-Phe-OMe, 1.5 equiv of Pybop, DCM, 2 h, 80.3%; (d) 1 N NaOH in MeOH, 30 min, 93.0%; (e) 2 N HCl in 1,4-dioxane, 3 h; (f) 3.0 equiv of HOBt, 3.0 equiv of EDC, 5.0 equiv of DIPEA, DCM, overnight, 32.8%; (g) 20% TFA in DCE, 1 h, 80.2%.

moiety which irreversibly forms a covalent adduct with the active site cysteine residue of HRV 3CP [18]. The ethyl propenoate Michael acceptor moiety corresponds to the P2′ position of AG7088 (boxed in compounds **9a**–**f** in Fig. 2). We reasoned that replacing this Michael acceptor moiety with one containing aromatic rings would significantly increase the inhibitory activity of the compound against CVB3 3CP, because the aromatic rings would provide additional hydrophobic or π–π interactions with Tyr22. An analog of AG7088 was synthesized (compound **9a**), which contains a glutamine residue instead of a lactam ring in the P1 position (shaded in compounds **9a**–**f**). This substitution greatly simplified the synthesis of the compounds. Five derivatives (**9b**–**f**) of AG7088 which contain various aromatic rings instead of the ethyl moiety at the P2′ position were synthesized (Fig. 2). Detailed procedures for

the synthesis of these derivatives are described in the Materials and methods.

Determination of IC_{50} values

IC_{50} values of the AG7088 analog and its derivatives were determined using purified recombinant CVB3 3CP *in vitro* (Table 1). Compound **9a**, an analog of AG7088, possessed moderate inhibitory activity against CVB3 3CP, which is consistent with previous reports assessing AG7088 [10]. All five derivatives containing aromatic rings at the P2′ position showed significantly enhanced inhibitory activities against CVB3 3CP, and the compound **9b** derivative carrying a naphthalene ring was the most efficient inhibitor with an IC_{50} value of 93 nM. These results demonstrate the validity of our rational approach for designing potent inhibitors of CVB3 3CP.

Antiviral activity assay

We examined whether inhibiting CVB3 3CP activity is able to prevent the proliferation of CVB3. None of the synthesized compounds had direct cytotoxicity when used at concentrations up to 100 μM (data not shown). In an initial experiment, compound **9b** showed the most prominent antiviral activity (data not shown), which was well correlated with its inhibition of the protease activity *in vitro*. Therefore, compound **9b** was analyzed further. HeLa-UVM cells were transfected with CVB3-H3 (MOI, 100) in the presence of various concentrations of compound **9b**, and cell viability was determined after 24 h. Compared to CVB3-H3 infected cultures incubated in the absence of compound **9b**, the viability was significantly greater in cultures incubated in the presence of 5–10 μM compound **9b**, and was completely restored to control levels in the presence of 50 μM compound **9b** (Fig. 3A). We then tested whether the recovery in viability in CVB3-H3 infected cultures that were incubated with compound **9b** was associated with the inhibition of CVB3 3CP activity. A CVB3 3CP-dependent GFP assay was performed as described previously [17]. HeLa-UVM cells were transfected with a GFP-CVB3 fusion construct in which a CVB3 3CP cleavage site is placed between GFP and the CVB3 polyprotein. Cleavage by CVB3 3CP releases the GFP from the fusion protein, which can be observed directly by fluorescence microscopy or by Western blotting. Compound **9b** significantly reduced the number of the GFP positive cells (Fig. 3B) and reduced the amount of GFP detected by Western blotting (Fig. 3C) in a dose dependent manner. These data indicate that compound **9b** inhibits CVB3 3CP activity and CVB3 proliferation *in vivo* in a dose-dependent manner.

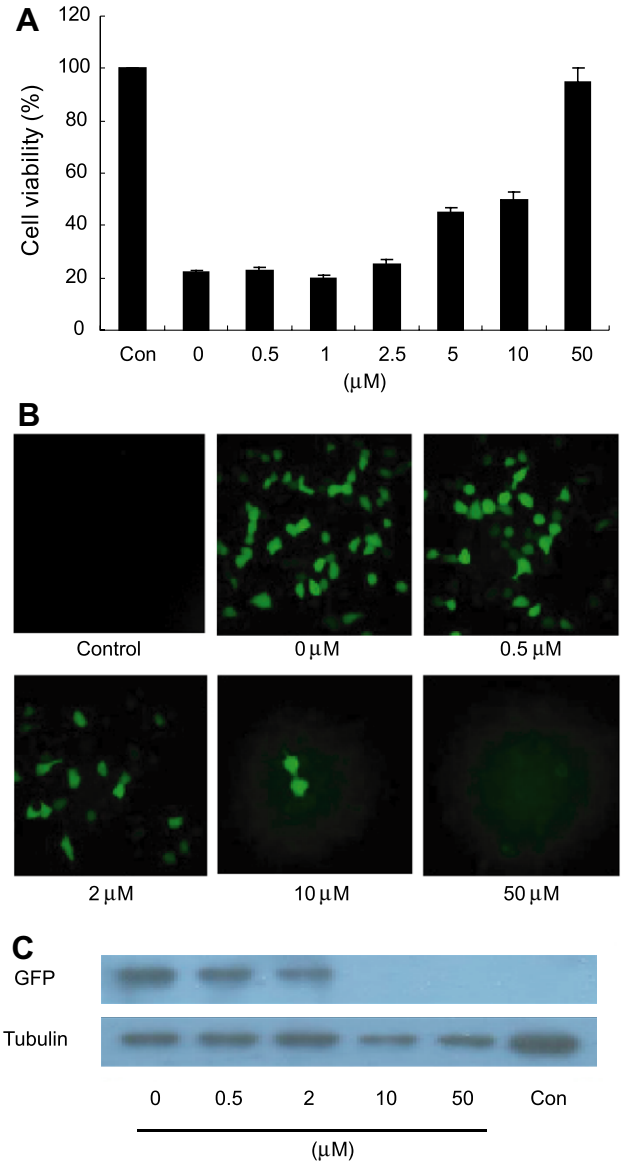

Fig. 3. Inhibition of viral proliferation by compound **9b**. (A) Antiviral activity of compound **9b**. HeLa-UVM cells were transfected with CVB3-H3 in the presence of various amounts of compound **9b** for 24 h. Cell viabilities are presented as means ± SD from three independent experiments. (B,C) Inhibition of CVB3 3CP by compound **9b**. HeLa cells were infected with GFP-CVB3 (MOI, 100), and treated with various amounts of compound **9b**. The CVB3 3CP activity was monitored by the expression of GFP using fluorescence microscopy (B), and Western blotting (C). Tubulin was used as a loading control.

Table 1
IC_{50} values

Compounds	R	Formula	IC_{50} (nM)
9a	CH_2CH_3	$C_{28}H_{36}FN_5O_7$	48,000
9b	$CH_2C_{10}H_7$	$C_{37}H_{40}FN_5O_7$	93
9c	$CH(C_6H_5)_2$	$C_{39}H_{42}FN_5O_7$	480
9d	$CH_2C_6H_5$	$C_{33}H_{38}FN_5O_7$	650
9e	$CH_2CH_2C_6H_5$	$C_{34}H_{40}FN_5O_7$	950
9f	$CH_2CH_2(p\text{-}F\text{-}C_6H_5)$	$C_{34}H_{39}F_2N_5O_7$	1000

Compound **9a** is an analog of AG7088, a potent inhibitor of HRV 3CP. Compounds **9b**–**f** are derivatives of AG7088 containing aromatic groups at the Michael acceptor position instead of an ethyl group.

In conclusion, we have successfully designed and synthesized a potent CVB3 3CP inhibitor using a structure-based rational design approach. This inhibitor will serve as a platform to generate more effective and specific CVB3 3CP

inhibitors and contribute to our understanding of the pathology of CVB3.

Acknowledgments

During this work, W.J.P. was supported by a GRL Grant (M6-0605-00-0001) from the Ministry of Science and Technology, Korea, YCK was supported by a grant of the Korea Health 21 R&D Project, from the Ministry of Health & Welfare, Republic of Korea (Grant No. A040042), and OKP was supported by a grant from the Plant Signaling Network Research Center funded by the Korea Science and Engineering Foundation.

References

[1] J. Yuan, D.A. Stein, T. Lim, D. Qiu, S. Coughlin, Z. Liu, Y. Wang, R. Bouch, H.M. Moulton, P.L. Iversen, D. Yang, Inhibition of Coxsackievirus B3 in cell-cultures and in mice by peptide-conjugated morpholino oligomers targeting the IRES, J. Virol. 79 (2006) 2151–2159.

[2] R. Zell, R. Markgraf, M. Schmidtke, M. Gorlach, A. Stelzner, A. Henke, H.H. Sigusch, B. Gluck, Nitric oxide donors inhibit the coxsackievirus B3 proteinases 2A and 3C in vitro, virus production in cells, and signs of myocarditis in virus-infected mice, Med. Microbiol. Immunol. 193 (2004) 91–100.

[3] S.A. Huber, A.M. Feldman, D. Sartini, Coxsackievirus B3 induces T regulatory cells, which inhibit cardiomyopathy in tumor necrosis factor-α transgenic mice, Circ. Res. 99 (2006) 1109–1116.

[4] D.H.W. Chau, J. Yuan, H. Zhang, P. Cheung, T. Lim, Z. Liu, A. Sall, D. Yang, Coxsackievirus B3 proteases 2A and 3C induce apoptotic cell death through mitochondrial injury and cleavage of eIF4GI but not DAP5/p97/NAT1, Apoptosis 12 (2007) 513–524.

[5] A. D'Ambrosioa, G. Pattia, A. Manzolia, G. Sinagrab, A. Di Lenardab, F. Silvestric, G. Di Sciascioa, The fate of acute myocarditis between spontaneous improvement and evolution to dilated cardiomyopathy: a review, Heart 85 (2001) 499–504.

[6] L. Tong, Viral proteases, Chem. Rev. 102 (2002) 4609–4626.

[7] M.S. Lall, R.P. Jain, J.C. Vederas, Inhibitors of 3C cysteine proteinases from Picornaviridae, Curr. Top. Med. Chem. 4 (2004) 1239–1253.

[8] E. Arnold, M.G. Rossmann, Analysis of the structure of a common cold virus, human rhinovirus 14, refined at a resolution of 3.0 A, J. Mol. Biol. 211 (1990) 763–801.

[9] A.T. Hadfield, W. Lee, R. Zhao, M.A. Oliveira, I. Mino, R.R. Rueckert, M.G. Rossmann, The refined structure of human rhinovirus 16 at 2.15 A resolution: implications for the viral life cycle, Structure 15 (1997) 427–441.

[10] A.K. Patick, S.L. Binford, M.A. Brothers, R.L. Jackson, C.E. Ford, M.D. Diem, F. Maldonado, P.S. Dragovich, R. Zhou, T.J. Prins, S.A. Fuhrman, J.W. Meador, L.S. Zalman, D.A. Matthews, S.T. Worland, *In vitro* antiviral activity of AG7088, a potent inhibitor of human rhinovirus 3C protease, Antimicrob. Agents Chemother. 43 (1999) 2444–2450.

[11] A. Sali, T.L. Blundell, Comparative protein modeling by satisfaction of spatial restraints, J. Mol. Biol. 234 (1993) 779–815.

[12] D.V.D. Spoel, E. Lindahl, B. Hess, G. Groenhof, A.E. Mark, H.J.C. Berendsen, GROMACS: fast, flexible and free, J. Comp. Chem. 26 (2005) 1701–1718.

[13] P.S. Dragovich, T.J. Prins, R. Zhou, S.A. Fuhrman, A.K. Patick, D.A. Matthews, J.W. Meador III, R.A. Ferre, S.T. Worland, Structure-based design, synthesis, and biological evaluation of irreversible human rhinovirus 3C protease inhibitors. 3. Structure–activity studies of ketomethylene-containing peptidomimetics, J. Med. Chem. 42 (1999) 1203–1212.

[14] M.G. Cordingley, R.B. Register, P.L. Callahan, V.M. Garsky, R.J. Colonno, Cleavage of small peptides in vitro by human rhinovirus 14 3C protease expressed in *Escherichia coli*, J. Virol. 63 (1989) 5037–5045.

[15] K.U. Knowlton, E.S. Jeon, N. Berkley, R. Wessely, S. Huber, A mutation in the puff region of VP2 attenuates the myocarditis phenotype of an infectious cDNA of the Woodruff variant of coxsackievirus B3, J. Virol. 70 (1996) 7811–7818.

[16] E.S. Jeon, B.K. Lim, S.C. Choe, *In vivo* myocardial gene transfer using recombinant coxsackievirus B3, Circulation 105 (2002) 1278–1281.

[17] B.K. Lim, J.O. Shin, D.J. Choi, D.K. Kim, S.C. Choe, K. Knowlton, E.S. Jeon, Long-term cardiac gene expression using a coxsackieviral vector, J. Mol. Cell. Cardiol. 38 (2005) 745–751.

[18] P.S. Dragovich, T.J. Prins, R. Zhou, S.E. Stephen, J.T. Marakovits, S.A. Fuhrman, A.K. Patick, D.A. Matthews, C.A. Lee, C.E. Ford, B.J. Burke, P.A. Rejto, T.F. Hendrickson, T. Tuntland, E.L. Brown, J.W. Meador III, R.A. Ferre, J.E.V. Harr, M.B. Kosa, S.T. Worland, Structure-based design, synthesis, and biological evaluation of irreversible human rhinovirus 3C protease inhibitors. 4. Incoporation of P_1 Lactam moieties as L-glutamine replacements, J. Med. Chem. 42 (1999) 1212–1224.

[19] W.L. DeLano, The PyMOL molecular graphics system, 2002. Available from: <http://www.pymol.org>.